U.S. GEOLOGICAL SURVEY
COMPUTER CONTRIBUTION

# ADEPT: A program to estimate depth to magnetic basement from sampled magnetic profiles

by

Jeffrey D. Phillips

U. S. Geological Survey
OPEN FILE REPORT 79-367



U.S. Geological Survey
Reston, Virginia
1978

CONTENTS

## ABSTRACT

A fortran program computes depth to magnetic basement from the spatially varying autocorrelation function of a sampled magnetic profile. The depth calculation assumes a particular form for the autocorrelation function, and this assumption is tested against the measured autocorrelation function in order to reject invalid depth estimates.

## INTRODUCTION

Magnetic basement, the contact between magnetic and nonmagnetic rocks, is a surface which is often of geologic interest. Its configuration can reveal much about the history, structure and economic potential of buried rocks. Recent advances in technology permit the automated determination of depth to magnetic basement. The computer program ADEPT described in this report uses Hilbert transforms and Burg autocorrelation techniques to estimate depths to magnetic basement from evenly sampled magnetic profiles. The theoretical basis for this program is presented by Phillips (1979) and is summarized in the following section. The results of the computation must be interpreted using convergence criteria. The discussion is divided into two parts: a description of the program i/o and an example of the interpretation procedure.

## THEORY

A two dimensional basement surface can be constructed by laminating together a large number of very thin vertical or near vertical dikes. The dikes are of infinite extent in the $\pm y$ and $+z$ directions and terminate at a depth $z_1(x)$ below the surface $z = 0$. Each dike has a magnetization intensity m which may differ from those of adjoining dikes. A cross section in the x-direction reveals the topography of the basement $z_1(x)$. The magnetization of the basement is expressed as $m(x)$.

The magnetic anomaly profile $h(x)$ observed at the surface $z = 0$ is the superposition of the anomalies produced by each thin dike. To estimate the depth $z_1$ as a function of x, a short window will be passed along the magnetic profile. Within this window the anomaly will be assumed to originate from sources at a single constant depth $z_1$. With this restriction, the magnetic anomaly can be represented as the convolution of the magnetization $m(x)$ and an impulse response $g(x)$ which is equivalent to the anomaly of a single dike at depth $z_1$. Consequently the autocorrelation $\phi_h(x)$ of the magnetic profile is given by the convolution of the autocorrelation $\phi_m(x)$ of the magnetization and the autocorrelation $\phi_g(x)$ of the impulse response.

The form of $\phi_g$ is known and $\phi_h$ can be calculated from the observed profile within the window. The form of $\phi_m$ is arbitrary, but practical equations for depth estimation result only if the magnetization of each dike is totally independent of all other

dikes ($\phi_m(x) = \delta(x)$), or if the mean magnetization of the basement is a constant, but the magnetization of each dike varies independently about this mean ($\phi_m(x) = \delta(x) + \text{constant}$).

In the first case each lag of the autocorrelation $\phi_h$ yields a depth estimate given by

$$z_{1n} = \frac{n\Delta x}{2} \sqrt{\frac{1}{1/\phi_n - 1}} \qquad (1)$$

where $\phi_n$ is the n-th lag of the autocorrelation of the magnetic profile (normalized such that $\phi_0=1$), and $\Delta x$ is the sample interval of the magnetic profile. In the second case, depth estimates are given by

$$z_n = \left[ \frac{(n+1)^2 z_{1\,n}^2 - n^2 z_{1\,n+1}^2}{2n + 1 + 4(z_{1\,n+1}^2 - z_{1\,n}^2) / \Delta x^2} \right]^{1/2} \qquad (2)$$

where $z_{1n}$, $z_{1n+1}$ are obtained from equation (1).

The application of equations (1) and (2) proceeds in two stages. In the primary stage, a window is centered on each sample point of the magnetic profile, and several lags of the autocorrelation function are computed for the data within the window. Using equation (1), a depth is estimated for each lag. The convergence of these depth estimates is the criterion used to test the validity of the assumed model, and thus the validity of the depth estimates themselves. If the depth estimates remain nearly the same for all lags, then the calculated autocorrelation function has the form of the theoretical autocorrelation function, and we can assume that both the model and the depth

estimates are valid. If the depth estimates become significantly shallower for higher lags, the calculated autocorrelation function is too sharply peaked to fit the model. This behavior suggests that the sources of the magnetic anomaly are three dimensional and the depth estimates should be rejected. Conversely, depth estimates which deepen significantly for higher lags are evidence for one dimensional (i.e. flat) topography or correlated magnetization. Again the model is invalid and the depth estimates should be rejected. In areas where the depth estimates converge, the first lag of the autocorrelation will always provide the most reliable depth at the center of the window.

In the secondary stage, the primary depth estimates from equation (1), whether valid or invalid, are plugged into equation (2). the result is a set of secondary depth estimates at each sample point of the magnetic profile. Since each secondary depth estimate is based upon two lags of the computed autocorrelation function, convergence of any two secondary depth estimates implies that at least three lags of the computed autocorrelation function have the proper form for equation (2) to be valid. Thus any two secondary depth estimates that converge are assumed to be valid. As with the primary depth estimates, the behavior of divergent secondary depth estimates can be used to identify three dimensional source regions.

## I/O DESCRIPTION

A listing of the fortran IV program ADEPT is given in

Appendix I. The documentation given in the text of the program is supplemented here. A sample output is given in Appendix IV.

Input to the program consists of:

TITLE: profile identification.

LX: the number of equi-spaced data points in the profile. The program can accomodate up to 923 points without redimensioning.

DELX: the sample interval. Ideally DELX should not be greater than one half the shallowest depth of interest. Estimated depths will be expressed in the same units as the sample interval, DELX.

IW: the number of points in the adaptive window. IW should be large enough to provide good statistical resolution, but small enough to ensure minimum loss of information near the ends of the profile. The smoothness of the estimated magnetic basement may increase as IW is increased to 2*zmax/DELX, where zmax is the maximum depth of interest. Beyond this point increases in IW will have little effect. In most situations IW=15 is a good starting value.

ILINE: equals 1 for removal of a least squares linear trend from the data. If ILINE does not equal 1 only the mean is removed from the data.

IPUN: equals 1 for punched output.

ASCAL: the ordinate scale factor to be used in plotting the magnetic anomaly profile. ASCAL is in units per

inch, and the total range of amplitudes plotted will be ±6.*ASCAL.

DSCAL: the ordinate scale factor to be used in plotting the depth estimates. DSCAL is in units per inch, and the total range of depths plotted will be 0. to 12.*DSCAL.

FMT: the format in which the magnetic profile is to be read from cards.

X: the array containing the profile.

Output of the program consists of:

TITLE: profile identification.

INPUT PARAMETERS: see input description.

PREDICTION FILTER AND PREDICTED EXTENSION: generated for internal use by the program. They can be ignored by the ordinary user.

PRIMARY RESULT: this is the result obtained using equation (1).

LOCATION: distance along the profile expressed in the same units as the sample interval, DELX.

ANOMALY: the observed profile after the removal of a mean or a linear trend.

HILBERT: the Hilbert transform of the profile.

DIF: the difference between DEPTH1 and DEPTH4. At the ends of the profile, where less than four depths are calculated, DIF has been estimated by linear extrapolation from the available depth estimates.

DEPTH1, DEPTH2, DEPTH3, DEPTH4: depth estimates obtained from the first through fourth lags of the autocorrelation function of the profile using equation (1).

PLOT OF THE MAGNETIC PROFILE: the profile runs down the plot, with distance given along the left side. The amplitude scale, indicated at the top of the plot, is equal to ASCAL.

PLOT OF THE PRIMARY SOLUTION: the right side represents zero depth (e.g. the flight elevation) and depth increases DSCAL units/inch to the left. Distance is given along the left side. Four overlapping functions, DEPTH1, through DEPTH4, are plotted.

SECONDARY RESULT: this is the result obtained using equation (2).

LOCATION: distance along the profile.

IFLAG: indicates which depth estimate is preferred at this location on the basis of convergence--IFLAG=1 for DEPTH1 or 2 for DEPTH2.

DIF: the smallest difference between pairs of the depth estimates. One member of the chosen pair is the preferred depth given by IFLAG.

DEPTH1, DEPTH2,...: depth estimates from equation (2).

PLOT OF THE SECONDARY SOLUTION: similar to the plot of the primary solution.

## METHOD OF THE PROGRAM

This section can be skipped by the ordinary user. It describes the organization of the computer program and assumes an understanding of the complete theory presented by Phillips (1979).

The first step in processing is the removal of the mean from the profile. This is accompanied by removal of a regional trend in the form of a least squares line if ILINE = 1.

Generation of the analytic signal proceeds in two stages. First the profile is extended off both ends using a Burg prediction filter (Ulrych and others, 1973). The noncritical length NCOEF of the filter is set to 16 in a DATA statement. Use of the prediction filter has the effect of smoothly driving the profile to zero outside the measurement interval, thus reducing end effects in the calculation of the Hilbert transform. The analytic signal XC is obtained through operations in the wavenumber domain (Claerbout, 1976, p.12,20-21,62). The prediction filter WE, and the portion of the analytic signal corresponding to the predicted extension are printed out following the transformation. When this extension has been added to the end of the profile, the result is a periodic function whose length is a power of two. The small discontinuity in this periodic function is located in the middle of the extension, far from the true ends of the data.

Next comes initialization of the output power vector V(I), and the first rows of the prediction error filter matrix A(1,I)

and the autocorrelation matrix R(1,I). In each, I is the index corresponding to location along the magnetic profile. The adaptive weight vectors, WE and WO, are initialized under the arbitrary assumption that the source depth is 2.*DELX. The weight vectors will be corrected for apparent source depth following the first depth estimate. Two weight vectors are required because both even and odd numbers of correlation statistics will need to be averaged about each point of the profile. Note that the sample interval DELX is ignored until the output stage of the program. Samples are assumed to be unit distance apart and depths are computed in corresponding units. This avoids numerical problems that arise with very small and very large values of DELX.

Adaptive processing starts with assignment of the data to the forward and backward error vectors F and B. Entering the main DO-loop, we begin determining autocorrelation lags and the corresponding depth estimates. These parameters are evaluated in odd-even pairs, with the odd numbered lags and depths being evaluated first. The current forward-backward crosspower terms FB and autopower terms AA are determined at each point of the profile. Weighted averages, XP and AP, of these terms provide the crosspower-autopower ratios within windows centered about points of the profile (C) and within windows centered midway between points of the profile (CM). Subroutine DEPTH uses C to determine the new prediction error filter, the new output power, and the next autocorrelation coefficient using an algorithm of

Claerbout (1976, p.160). The current depth estimate D(I,IK) at the midpoint of the window is calculated using equation (1). The new depth is used to update the adaptive weights, and CM is used to obtain new forward and backward error terms through prediction error filtering. This process is repeated until a depth has been obtained at each point of the profile excepting the very ends where no reliable estimate is possible.

The second half of the main DO-loop repeats this procedure for the even numbered autocorrelation lag and associated parameters. The main difference is that the same crosspower-autopower ratio is used both to determine depth and to perform the prediction error filtering. This is possible because both the depth estimates and the filtering operations are centered on points of the profile for even numbered lags. At the end of the main DO-loop, two depth estimates have been obtained at each point of the profile. This loop is repeated until NC depth estimates have been obtained at each point. Altering NC from the present value of 4 to a higher multiple of two would require redimensioning of the arrays.

At the output stage, AA is filed with absicca values and V contains DIF, the difference between the first and final lag depth estimates. This is to be used in interpreting the results.

Following output of the primary results, the magnetic anomaly profile and the depth estimates are plotted. The depth estimates are then used to obtain the secondary solution (equation (2)). Here DIF is the minimum difference between pairs

of depth estimates and IFLAG is the index of the depth estimate corresponding to this minimum. The program ends after printing and plotting the secondary results.

When noisy data is to be analysed equation (A-1) of Phillips (1979) can be substituted for the equations used above. Appendix II contains the program modifications required for noisy data.

## INTERPRETATION OF RESULTS

Interpreted computer output for profile B-25 is presented in Appendix IV. This example will be used to illustrate the interpretation technique.

A typical interpretation procedure might begin with examination of the plotted depth estimates for the primary and secondary solutions. In the case of the primary solution we have four superimposed curves of depth vs. distance. Each curve represemts depths obtained from a different lag of the autocorrelation function of the magnetic profile. Where the four curves converge, we have valid depth estimates. Where they diverge, the data do not fit our theoretical model and we are unable to estimate source depth. A preliminary selection of valid depth estimates can be made directly on the printer plot. This has been done in the example by circling all points at which the four curves converge to within one raster (spacing unit) of the printer. This preliminary interpretation can be modified later by increasing or decreasing the allowable amount of convergence.

In a similar way, a preliminary selection of valid depth estimates can be made directly on the printer plot of the secondary solution. In this plot there are three superimposed curves of depth vs. distance. Valid depths are indicated by convergence of any two of these curves. Points at which two depth estimates lie within one raster of each other are circled in the example.

We now have two preliminary sets of valid depth estimates which are based upon an arbitrary choice of convergence interval (one raster). The final interpretation will be constructed by adjusting the acceptable ranges of convergence until the two solutions can be superimposed without disagreement.

At this stage we turn to the listings of the solutions. For the primary solution we are concerned with the columns labeled DISTANCE, DIF, and DEPTH1. The DIF column contains the difference between DEPTH1 and DEPTH4, the first and fourth lag depth estimates. Where this DIF value is close to zero, the depth estimate given by DEPTH1 is likely to be valid. Our job is to choose two thresholds such that DIF values falling between the thresholds indicate valid depth estimates in the DEPTH1 column.

For the secondary solution we are concerned with all of the columns except DEPTH3. Here DIF is the minimum difference between pairs of the three depth estimates: DEPTH1, DEPTH2 and DEPTH3. IFLAG equals one if DEPTH1 is one member of the convergent pair, otherwise IFLAG equals two. When DIF is close to zero the depth estimate given by DEPTH1 (if IFLAG is one) or

DEPTH2 (if IFLAG is two) is likely to be valid. Here, as with the primary solution, we must choose two threshold values for DIF such that a DIF value falling between the thresholds indicates a valid DEPTH1 or DEPTH2.

At the bottom of figure 1 we have plotted DEPTH1 vs. DISTANCE for the primary solution (solid curve) and DEPTH(IFLAG) vs. DISTANCE for the secondary solution (dashed curve). DEPTH(IFLAG) is defined as DEPTH1 if IFLAG = 1 and DEPTH2 if IFLAG = 2. We are fortunate that the two curves cross at several points. If this were not the case, we would be forced to base our interpretation on an arbitraay convergence interval such as the one we used in looking at the printer plots. Even with overlapping solutions, the choice of optimum thresholds can be a difficult process. Fortunately, in practical applications we can often settle for less than optimum results.

At the top of figure 1 we have plotted DIF vs. DISTANCE for the primary solution. Around km 14 in this curve we see that DIF goes strongly positive, indicating invalid depth estimates over a three dimensional source. If we specify DIF < 0.2 for the primary solution, we can remove most of this peak in the DIF vs. DISTANCE curve.

The primary and secondary solutions (figure 1) have crossovers at kms 6.5, 24.5, 35, 43.5 and 49.5. Because the two solutions are roughly similar, it can be assumed that there is only one magnetic basement. Therefore where the two solutions cross, one should become valid as the other becomes invalid. The

crossovers usually occur where the DIF vs. DISTANCE curve for the primary solution is crossing zero. This implies that DIF > 0.0 might be another requirement for the valid depths of the primary solution. A less severe cutoff of DIF > -0.1 is suggested by the fact that at one crossover (km 24.5) the primary solution has a DIF value of around -0.08.

At the bottom of figure 2 we have again plotted DEPTH(IFLAG) vs. DISTANCE for the secondary solution (dashed curve) as well as the portions of the DEPTH1 vs. DISTANCE curve for the primary solution which satisfy -0.1 < DIF < 0.2 (solid curves). The DIF vs. DISTANCE curve for the secondary solution is shown at the top of the figure. Because we are hypothesizing a single basement, we expect the secondary solution to be invalid where the primary solution is valid and vice versa. If we were to drop horizontal and vertical lines from the ends of the primary solution segments in figure 2 to the secondary solution curve, we would expect the cutoff in the secondary solution to lie along the part of the dashed curve between the horizontal nnd vertical lines. It follows that the DIF value of the lower cutoff would lie between -0.10 and +0.01 near km 12, between -0.19 and -0.03 near km 18, and between -0.13 and -0.06 near km 35. Thus any lower cutoff between -0.10 and -0.06 would satisfy our requirements near these points. This approach gives no reliable lower cutoffs near kms 24 and 43, where two basements may be present. The approach also gives no information on an upper bound for DIF.

Between kms 25 and 34 the primary solution is definitely

invalid and we are tempted to accept the secondary solution. However, the DIF values here are the largest positive values for the secondary solution, indicating a possible three dimensional source. The second highest peak in the DIF values for the secondary solution is around km 45. These dif values are also positive, but much less so. If we require DIF < 0.06 we are able to include these depths while discarding the questionable depths between kms 24 and 32. Retaining only depths we are certain of, we have valid secondary solutions in the range $-0.06 < DIF < 0.06$.

Figure 3 shows the basement obtained by combining the valid depths of the primary and secondary solutions. Regions where depth estimates have been rejected due to three dimensional behavior (DIF > 0.2 for the primary solution and DIF > 0.06 for the secondary solution) have been indicated by brackets at the top of the figure. Although there are some erroniously shallow depths near kms 24 and 32, the estimated magnetic basement agrees quite well with the acoustic basement known from a seismic reflection profile (Phillips, 1979). Clearly recognizible on the basement cross section are the shallowing of the basin to the right, the seamount near km 15 and its adjacent sedimentary troughs.

It is often possible to check the estimated magnetic basement by constructing two dimensional models which reproduce the observed magnetic profile. This is recommended in areas where no independent confirming evidence is available.

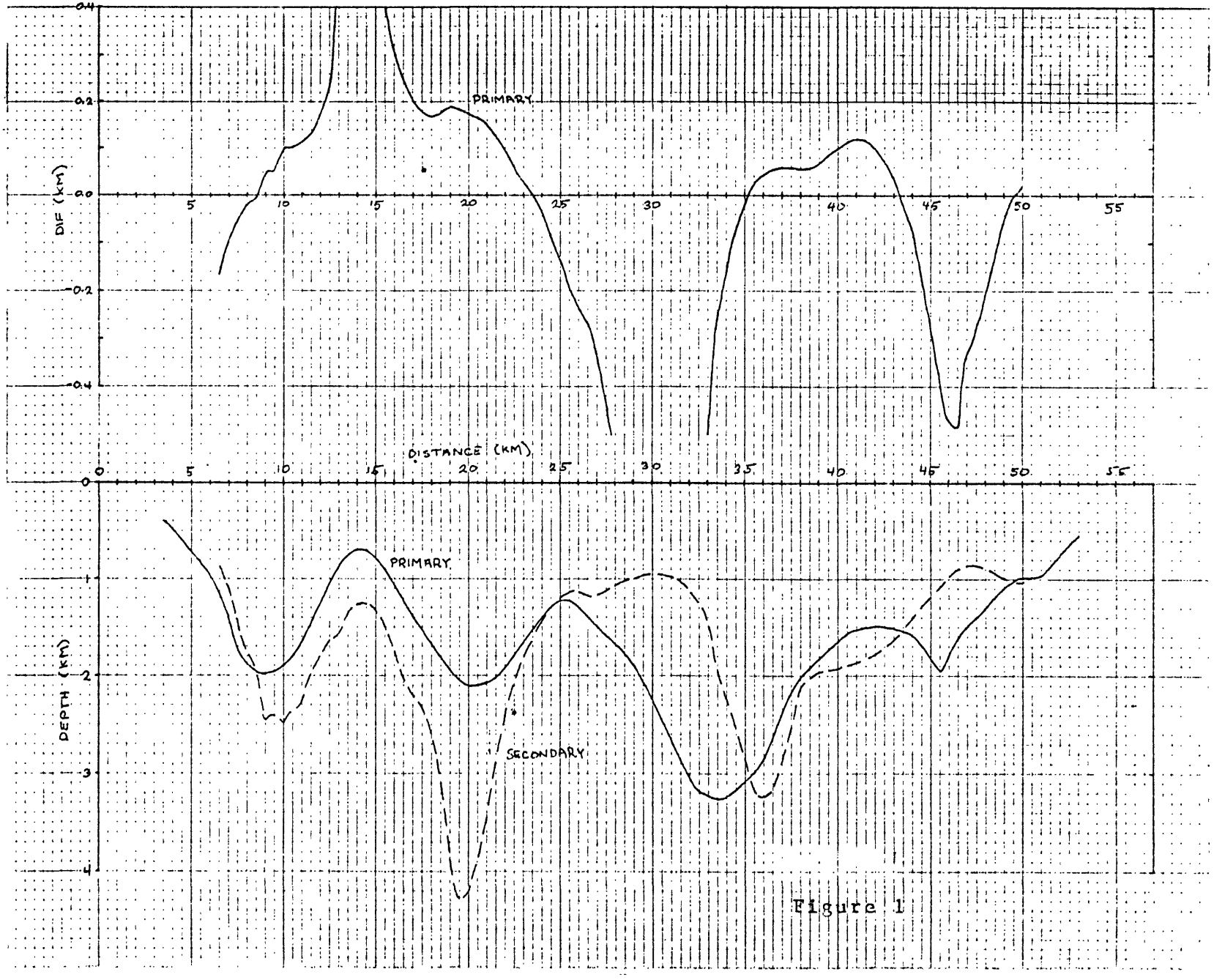
PRIMARY
DIF (KM)
0.4
0.2
0.0
-0.2
-0.4
5
10
15
20
25
30
40
45
50
55
DISTANCE (KM)
0
5
10
15
20
25
30
35
40
45
50
55
PRIMARY
SECONDARY
DEPTH (KM)
1
2
3
4

Figure 1

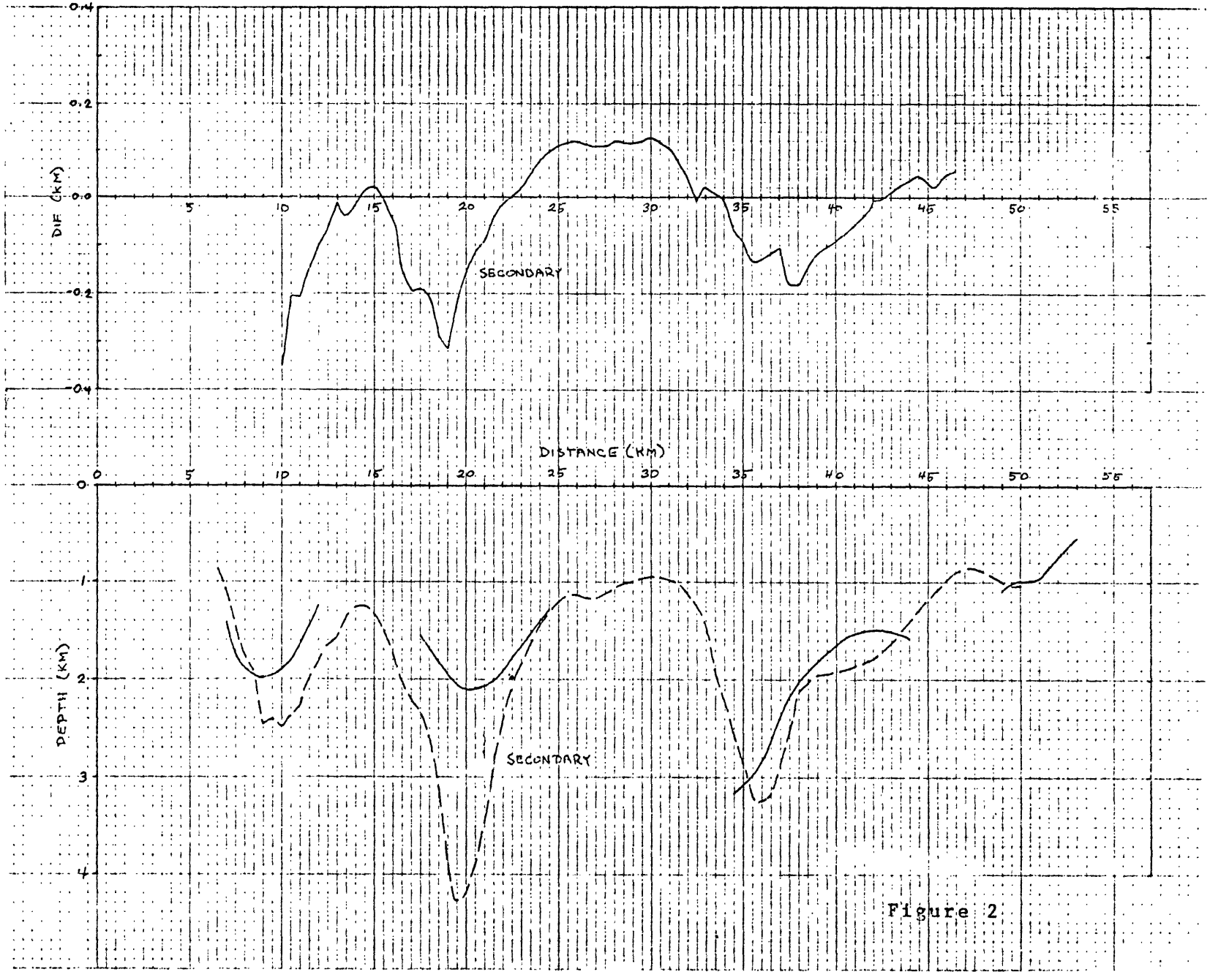
0.4
0.2
0.0
-0.2
-0.4
DIF (KM)
5
10
15
20
25
30
35
40
45
50
55
SECONDARY
DISTANCE (KM)
0
5
10
15
20
25
30
35
40
45
50
55
0
1
2
3
4
DEPTH (KM)
SECONDARY

Figure 2

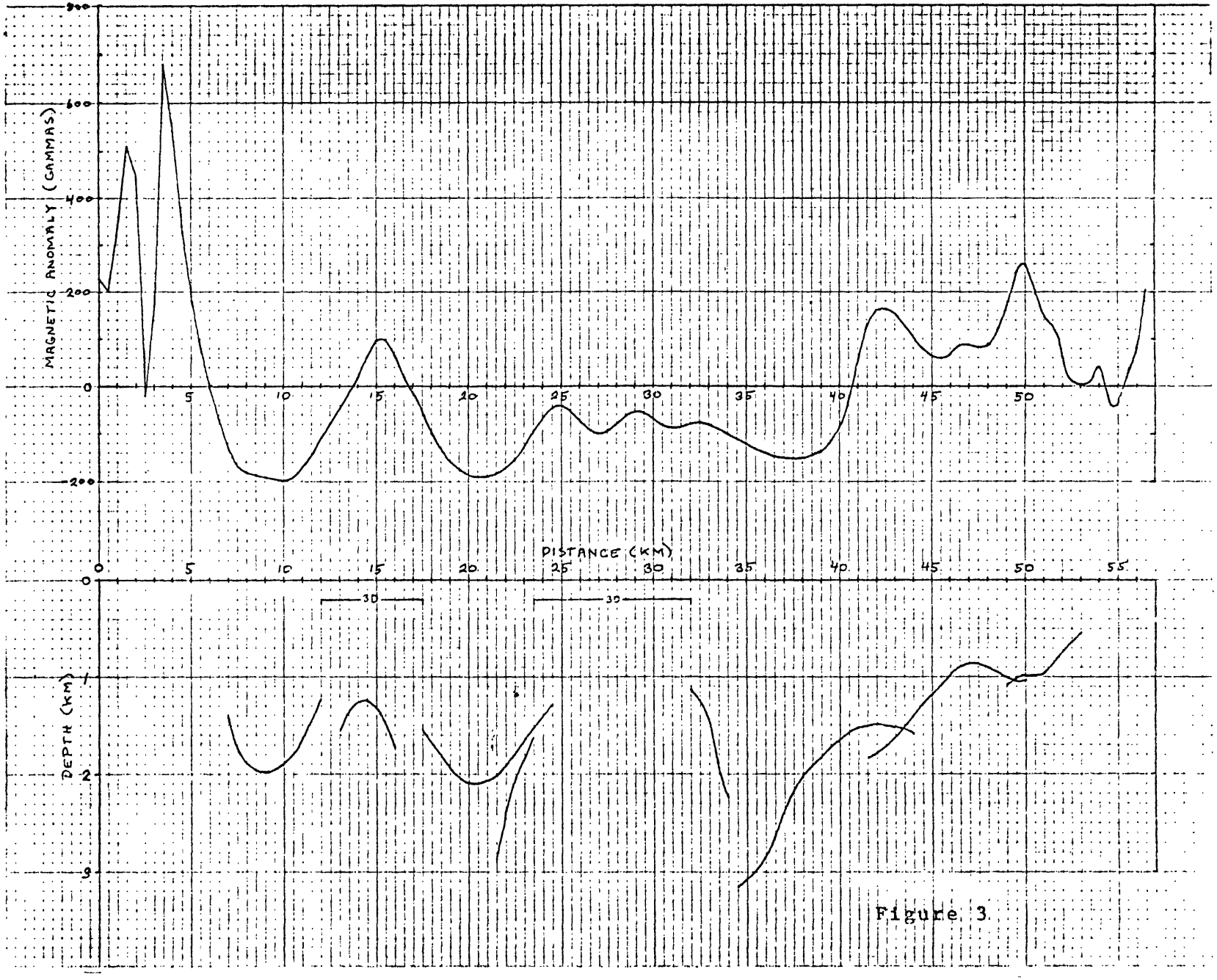
MAGNETIC ANOMALY (GAMMAS)
600
400
200
0
-200
5
10
15
20
25
30
35
40
45
50
DISTANCE (KM)
55
DEPTH (KM)
1
2
3

Figure 3.

## REFERENCES CITED

Claerbout, J. F., 1976, Fundamentals of Geophysical Data Processing With Applications to Petroleum Prospecting, McGraw-Hill, Inc., New York, pp. 12, 20-21, 62, 133-137, 160.

Phillips, J. D., 1979, Autocorrelation depth analysis of magnetic profiles, Geophysics, 44, in press.

Ulrych, T. J., Smylie, D. E., Jensen, O. G., and Clarke, G. K., 1973, Predictive filtering and smoothing of short records by using maximum entropy, J. Geophys. Res., 78, p. 4959-4964.

# APPENDIX I

## SOURCE PROGRAM LISTING

```
C     ********  PROGRAM ADEPT  ********
C     ESTIMATES DEPTH TO MAGNETIC BASEMENT FROM SAMPLED MAGNETIC PROFILES.
C     RESULTS MUST BE INTERPRETED USING THE CONVERGENCE OF THE DEPTH ESTIMATES.
C     SUBROUTINES REQUIRED:  DEPTH, FORK, DPLOT.
C     ORDER OF INPUT CARDS:
C     CARD 1:    TITLE              FORMAT(18A4)
C     CARD 2:    DELX,LX,IW,ILINE,IPUN  FORMAT(F10.7,4I5)
C     CARD 3:    ASCAL,DSCAL        FORMAT(2F10.2)
C     CARD 4:    (FMT)              FORMAT(18A4)
C     CARD 5:    X(I),I=1,LX        FORMAT(FMT)
C     WRITTEN BY J.PHILLIPS.
      COMMON A(5,1024),R(5,1024),V(1024),D(4,1024),ND(1024),C
      COMPLEX A,R,C,XC(1024),F(1024),B(1024),FB(1024),FTEM,CONJG,CM
      COMPLEX*16 XP
      REAL X(1024),D,TITLE(18),AA(1024),WE(50),WO(49),FMT(18)
      REAL*8 AP,XIND,DET,SQIS
      DATA NCOEF/16/
      NC=4
      READ(5,100) TITLE
      WRITE(6,100) TITLE
      READ(5,101) DELX,LX,IW,ILINE,IPUN
      WRITE(6,102) DELX,LX,IW,ILINE,IPUN
      READ(5,103) ASCAL,DSCAL
      READ(5,100) FMT
      READ(5,FMT)(X(I),I=1,LX)
  100 FORMAT(18A4)
  101 FORMAT(F10.7,4I5)
  102 FORMAT(1H0,'INPUT PARAMETERS',/,'   DELX=',F10.7,'   LX=',I5,
     1       '   IW=',I5,'   ILINE=',I5,'   IPUN=',I5,
     2       //,' PREDICTION FILTER',/)
  103 FORMAT(2F10.2)
      LXM1=LX-1
      SLOPE=0.
      DB=0.
      DO 5 I=1,LX
    5 DB=DB+X(I)
      DB=DB/LX
      IF(ILINE.NE.1) GO TO 11
      SLOPE=(X(LX)-X(1))/LXM1
      DB=X(1)
      DO 6 I=1,LX
    6 X(I)=X(I)-(I-1)*SLOPE-DB
C   REMOVE LEAST SQUARES LINE
      ISUM=LXM1*LX/2
      SQIS=LXM1*LX*(LX+LX-1)/6
      XIND=0.
      XSUM=X(LX)
      DO 10 I=1,LXM1
      XIND=XIND+X(I+1)*I
   10 XSUM=XSUM+X(I)
      DET=LX*SQIS-ISUM*ISUM
      SLOPE=(LX*XIND-ISUM*XSUM)/DET
      DB=(SQIS*XSUM-ISUM*XIND)/DET
   11 CONTINUE
```

```
      DO 12 I=1,LX
      X(I)=X(I)-(I-1)*SLOPE-DB
   12 XC(I)=X(I)
C  DETERMINE PREDICTION FILTER
      DO 20 I=1,LX
      AA(I)=X(I)
   20 V(I)=X(I)
      WE(1)=1.
      DO 23 J=2,NCOEF
      AP=0.
      XIND=0.
      DO 21 I=J,LX
      AP=AP+AA(I)*AA(I)+V(I-J+1)*V(I-J+1)
   21 XIND=XIND+AA(I)*V(I-J+1)
      RC=-2.*XIND/AP
      DO 22 I=J,LX
      TEMP=AA(I)
      AA(I)=AA(I)+RC*V(I-J+1)
   22 V(I-J+1)=V(I-J+1)+RC*TEMP
      WE(J)=0.
      JH=(J+1)/2
      DO 23 I=1,JH
      K=J-I+1
      TEMP=WE(K)+RC*WE(I)
      WE(I)=WE(I)+RC*WE(K)
   23 WE(K)=TEMP
C  EXTEND PROFILE
      K=LX+100
      DO 24 I=1,11
      LC=2**I
      IF(LC.GT.K) GO TO 25
   24 CONTINUE
   25 LP=LX+1
      JH=(LP+LC)/2
      DO 26 I=LP,JH
      XC(I)=0.
      XC(LC-I+LP)=0.
      DO 26 J=2,NCOEF
      XC(I)=XC(I)-WE(J)*XC(I-J+1)
   26 XC(LC-I+LP)=XC(LC-I+LP)-WE(J)*XC(MOD(LC-I+LP+J-2,LC)+1)
C  BEGIN HILBERT TRANSFORM
      CALL FORK(LC,XC,-1.)
      K=LC/2
      DO 30 J=2,K
      XC(J)=XC(J)+XC(J)
   30 XC(LC+2-J)=0.
      CALL FORK(LC,XC,+1.)
C  END HILBERT TRANSFORM
      WRITE(6,104)(WE(J),J=1,NCOEF)
      WRITE(6,105)
      WRITE(6,106)(XC(I),I=LP,LC)
  104 FORMAT(12F10.7)
  105 FORMAT(1H0,'PREDICTED EXTENSION',//)
  106 FORMAT(12F10.2)
```

```
      DO 40 I=1,LX
      V(I)=1.
      A(1,I)=1.
      R(1,I)=1.
      DO 40 J=1,NC
   40 D(J,I)=0.
      IS=IW/2
      IW=IS+IS+1
      IWM1=IW-1
      IWM2=IW-2
      IWM3=IW-3
      IWP1=IW+1
      ISP1=IS+1
      LXMS=LX-IS
      LMSP=LXMS+1
C  INITIALIZE WEIGHTS
      ZE=4.
      DO 41 J=1,IS
      RO=J-IS
      RE=RO-0.5
      WO(J)=RO*RO+ZE
      WO(IWM1-J)=WO(J)
      WE(J)=RE*RE+ZE
   41 WE(IW-J)=WE(J)
      DXS=ZE
C  BEGIN ADAPTIVE PROCESSING
      DO 42 J=1,LX
      F(J)=XC(J)
   42 B(J)=XC(J)
C  ENTER MAIN LOOP
      DO 52 I=1,NC,2
      IP=I+1
      IB=(I-1)*IS+2
      IE=LX-IB+I+1
      DO 43 J=IB,IE
      FB(J)=F(J)*CONJG(B(J-I))
   43 AA(J)=F(J)*CONJG(F(J))+B(J-I)*CONJG(B(J-I))
      IE=IE-IWM2
      DO 48 K=IB,IE
      XP=0.
      AP=0.
      DO 44 J=1,IWM2
      XP=XP+FB(K+J-1)/WO(J)
   44 AP=AP+AA(K+J-1)/WO(J)
      CM=(XP+XP)/AP
      XP=0.
      AP=0.
      DO 45 J=1,IWM1
      XP=XP+FB(K+J-1)/WE(J)
   45 AP=AP+AA(K+J-1)/WE(J)
      C=(XP+XP)/AP
      IK=K+IS-IP/2
      CALL DEPTH(I,IK)
C  SET WEIGHTS
```

```
      ZP=D(I,IK)*D(I,IK)
      IF(ZP.LT.DXS) ZP=DXS
      DO 46 J=1,IWM1
   46 WE(J)=WE(J)-ZE+ZP
      DO 47 J=1,IWM2
   47 WO(J)=WO(J)-ZE+ZP
      ZE=ZP
      IK=IK+I/2
      FTEM=F(IK)
      F(IK)=F(IK)-CM*B(IK-I)
   48 B(IK-I)=B(IK-I)-CONJG(CM)*FTEM
      IK=IK+IP/2
      F(IK)=F(IK)-C*B(IK-I)
      IB=IB+IS
      IE=IE+IS
      DO 49 J=IB,IE
      FB(J)=F(J)*CONJG(B(J-IP))
   49 AA(J)=F(J)*CONJG(F(J))+B(J-IP)*CONJG(B(J-IP))
      IE=IE-IWM3
      DO 52 K=IB,IE
      XP=0.
      AP=0.
      DO 50 J=1,IWM2
      XP=XP+FB(K+J-1)/WO(J)
   50 AP=AP+AA(K+J-1)/WO(J)
      C=(XP+XP)/AP
      IK=K+IS-IP/2-1
      CALL DEPTH(IP,IK)
C  SET WEIGHTS
      ZP=D(IP,IK)*D(IP,IK)
      IF(ZP.LT.DXS) ZP=DXS
      DO 51 J=1,IWM2
   51 WO(J)=WO(J)-ZE+ZP
      ZE=ZP
      IK=IK+IP/2
      FTEM=F(IK)
      F(IK)=F(IK)-C*B(IK-IP)
   52 B(IK-IP)=B(IK-IP)-CONJG(C)*FTEM
C  PROCESSING COMPLETED
C  BEGIN OUTPUT
      WRITE(6,107)
      DO 60 I=1,IS
      AA(I)=(I-1)*DELX
   60 WRITE(6,108) AA(I),XC(I)
      DO 62 I=ISP1,LXMS
      AA(I)=(I-1)*DELX
      J=ND(I)
      DO 61 K=1,J
   61 D(K,I)=D(K,I)*DELX
      V(I)=3.*(D(1,I)-D(J,I))/(FLOAT(J-1)+.1E-05)
   62 WRITE(6,108) AA(I),XC(I),V(I),(D(K,I),K=1,J)
      DO 63 I=LMSP,LX
      AA(I)=(I-1)*DELX
   63 WRITE(6,108) AA(I),XC(I)
```

```
      CALL DPLOT(X,1,1,LX,1,2,DELX,ASCAL,0.)
      CALL DPLOT(D,4,NC,LX,-1,1,DELX,DSCAL,0.)
  107 FORMAT(1HO,'PRIMARY RESULT',//,'  LOCATION',5X,'ANOMALY',3X,
     1       'HILBERT',4X,'DIF',6X,'DEPTH1',3X,'DEPTH2...'/)
  108 FORMAT(2H  ,F7.2,2X,2F10.2,3X,F7.3,6(3X,F6.3))
      IF(IPUN.EQ.1) WRITE(7,111)(AA(I),XC(I),D(1,I),V(I),I=1,LX)
C   OBTAIN SECONDARY RESULT
      WRITE(6,109)
      DXS=DELX*DELX
      ISP1=IS+IS
      LXMS=LX-ISP1+1
      DO 75 K=ISP1,LXMS
      N=ND(K)
      DO 70 I=1,N
   70 WE(I)=D(I,K)*D(I,K)
      D(N,K)=0.
      N=N-1
      DO 71 I=1,N
      IP=I+1
      IP2=IP*IP
      I2=I*I
      ARG=(IP2*WE(I)-I2*WE(IP))/(IP2-I2+4.*(WE(IP)-WE(I))/DXS)
      IF(ARG.LT.0.) ARG=0.
      D(I,K)=SQRT(ARG)
   71 CONTINUE
      AA(K)=(K-1)*DELX
      IFLAG=1
      IF(N.GT.2) GO TO 72
      V(K)=D(1,K)-D(N,K)
      GO TO 74
   72 V(K)=D(1,K)-D(2,K)
      NM1=N-1
      DO 73 I=1,NM1
      IP1=I+1
      DO 73 J=IP1,N
      CS=D(I,K)-D(J,K)
      IF(ABS(CS).GT.ABS(V(K))) GO TO 73
      V(K)=CS
      IFLAG=I
   73 CONTINUE
   74 ND(K)=IFLAG
   75 WRITE(6,110) AA(K),IFLAG,V(K),(D(I,K),I=1,N)
      NC=NC-1
      CALL DPLOT(D,4,NC,LX,-1,1,DELX,DSCAL,0.)
  109 FORMAT(1HO,'SECONDARY RESULT',//,'  LOCATION',1X,
     1       'FLAG',5X,'DIF',5X,'DEPTH1',3X,'DEPTH2...'/)
  110 FORMAT(2H  ,F7.2,I5,3X,F7.3,4(3X,F6.3))
      IF(IPUN.EQ.1) WRITE(7,112)(AA(K),D(ND(K),K),V(K),K=ISP1,LXMS)
  111 FORMAT(5F10.3)
  112 FORMAT(6F10.3)
      STOP
      END
```

```
      SUBROUTINE DEPTH(I,IK)
      COMMON A(5,1024),R(5,1024),V(1024),D(4,1024),ND(1024),C
      COMPLEX A,R,C,BOT,CONJG
C   DETERMINE NEW AUTOCORRELATION COEFFICIENT
      IP=I+1
      A(IP,IK)=0.
      R(IP,IK)=C*V(IK)
      V(IK)=V(IK)*(1.-C*CONJG(C))
      DO 20 J=2,IP
   20 R(IP,IK)=R(IP,IK)-A(J,IK)*R(IP-J+1,IK)
      IG=(IP+1)/2
      DO 21 J=1,IG
      BOT=A(IP-J+1,IK)-C*CONJG(A(J,IK))
      A(J,IK)=A(J,IK)-C*CONJG(A(IP-J+1,IK))
   21 A(IP-J+1,IK)=BOT
C   DETERMINE DEPTH
C     ARG=(2*I-1)/(REAL(R(I,IK))/REAL(R(IP,IK))-1.)-(I-1)*(I-1)
      ARG=I*I/(1./REAL(R(IP,IK))-1.)
      IF(ARG.LT.0.) ARG=0.
      D(I,IK)=0.5*SQRT(ARG)
      ND(IK)=I
      RETURN
      END
```

```
      SUBROUTINE FORK(LX,CX,SIGNI)
C
C                          LX
C   CX(K) = SQRT(1/LX)  SUM (CX(J)*EXP(2*PI*SIGNI*I*(J-1)*(K-1)/LX))
C                       J=1
C
C                                    FOR K=1,2,...,(LX=2**INTEGER)
C   WRITTEN BY J.F.CLAERBOUT.
      COMPLEX CX(LX),CARG,CEXP,CW,CTEMP
      J=1
      SC=SQRT(1./LX)
      DO 5 I=1,LX
      IF(I.GT.J)GO TO 2
      CTEMP=CX(J)*SC
      CX(J)=CX(I)*SC
      CX(I)=CTEMP
    2 M=LX/2
    3 IF(J.LE.M)GO TO 5
      J=J-M
      M=M/2
      IF(M.GE.1)GO TO 3
    5 J=J+M
      L=1
    6 ISTEP=2*L
      DO 8 M=1,L
      CARG=(0.,1.)*(3.14159265*SIGNI*(M-1))/L
      CW=CEXP(CARG)
      DO 8 I=M,LX,ISTEP
      CTEMP=CW*CX(I+L)
      CX(I+L)=CX(I)-CTEMP
    8 CX(I)=CX(I)+CTEMP
      L=ISTEP
      IF(L.LT.LX)GO TO 6
    9 RETURN
      END
```

```
      SUBROUTINE DPLOT(F,NDIM,N,M,JSIGN,NSIDE,DELX,SCALE,FILL)
C     A HIGH DENSITY PRINTER PLOT ROUTINE.  SUCCESSIVE VALUES ARE PLOTTED AS
C     APOSTROPHES AND PERIODS UNLESS THEY OCCUPY THE SAME SPACE IN WHICH CASE
C     A VERTICAL SLASH IS USED.
C
C         JSIGN = +1 FOR POSITIVE UP
C               = -1 FOR POSITIVE DOWN
C         NSIDE =  1 FOR ONE SIDED INPUT
C                  2 FOR TWO SIDED INPUT
C         FILL  =  1. FOR NO OVERLAP
C                  0. FOR TOTAL OVERLAP
C         SCALE =  UNITS/INCH
C
C     WRITTEN BY D.C.RILEY AND MODIFIED BY J.PHILLIPS.
      DIMENSION F(NDIM,M)
      INTEGER LINE(121),LINE1(121),ITEML(9),ITEMR(9)
      DATA IL,IR,IM,IB,LINE/4H''''','....','||||',122*'     '/
      DATA LINE1/121*'----'/
      WRITE(6,904) SCALE
      WRITE(6,906) LINE1
      SC=10.*JSIGN/SCALE
      ISET=61-JSIGN*60
      IF(NSIDE.EQ.2) ISET=61-FILL*JSIGN*(60-120/(2*N))
      IBIAS=120*FILL*JSIGN/N
      DO 16 K=2,M,2
      DO 11 J=1,N
      IMAGL=ISET+(J-1)*IBIAS
      LINE(IMAGL)=IM
      IMAGL=MIN0(MAX0(1,IFIX(F(J,K-1)*SC)+ISET+(J-1)*IBIAS),121)
      ITEML(J)=IMAGL
   11 LINE(IMAGL)=IL
      DO 13 J=1,N
      IMAGR=MIN0(MAX0(1,IFIX(F(J,K)*SC)+ISET+(J-1)*IBIAS),121)
      ITEMR(J)=IMAGR
      IF(LINE(IMAGR).EQ.IR) GO TO 13
      IF(LINE(IMAGR).NE.IB) GO TO 12
      LINE(IMAGR)=IR
      GO TO 13
   12 LINE(IMAGR)=IM
   13 CONTINUE
      IF(MOD(K-2,10).EQ.0) GO TO 14
      WRITE(6,907) LINE
      GO TO 15
   14 XL=(K-2)*DELX
      WRITE(6,908) XL,LINE
   15 CONTINUE
      DO 16 J=1,N
      LINE(ITEML(J))=IB
   16 LINE(ITEMR(J))=IB
      WRITE(6,906) LINE1
      DO 17 J=1,N
      IMAGL=ISET+(J-1)*IBIAS
   17 LINE(IMAGL)=IB
      RETURN
  904 FORMAT(1H1,50X,F8.3,' UNITS/INCH'/)
  906 FORMAT(10X,121A1)
  907 FORMAT(9X,'|',121A1,'|')
  908 FORMAT(1H ,F8.3,'+',121A1,'+')
      END
```

## APPENDIX II

## MODIFICATIONS FOR NOISY DATA

When the magnetic profile is contaminated by measurement rrors or noise, the computer program may need to be modified. ossible modifications presented here include low pass filtering nd substitution of a new depth formula.

Low pass filtering of the magnetic profile can be performed uring the Hilbert transformation. For example, the following ode could be substituted to remove power at wavenumbers greater han 3/4 the Nyquist.

```
C  BEGIN HILBERT TRANSFORM
      CALL FORK(LC,XC,-1.)
      K=LC/4
      DO 30 J=2,K
      XC(J)=XC(J)+XC(J)
   30 XC(LC+2-J)=0.
      K=K+1
      L=LC/2+1
      DO 31 J=K,L
      ARG=3.14159265*FLOAT(J-K)/(L-K)
      XC(J)=XC(J)*(1.+COS(ARG))
   31 XC(LC+2-J)=0.
      CALL FORK(LC,XC,+1.)
C  END HILBERT TRANSFORM
```

For noisy data, equation (A-1) of Phillips (1979) can be ubstituted for equation (1). This is accomplished by replacing he expression for ARG in subroutine DEPTH by the alternate xpression contained in the preceeding comment card. This change n depth formulas must be accompanied by a change in output. DIF alues must be calculated for each pair of depth esstimates at a iven point, and the best depth must be flagged. A secondary olution cannot be obtained. These changes are accomplished by ubstitutuon of the following output stage.

```
C  BEGIN OUTPUT
      CALL DPLOT(X,1,1,LX,1,2,DELX,ASCAL,0.)
      WRITE(6,107)
      DO 60 I=1,IS
      X(I)=0.
      AA(I)=(I-1)*DELX+XSTART
   60 WRITE(6,108) AA(I),XC(I)
      DO 65 I=ISP1,LXMS
      AA(I)=(I-1)*DELX+XSTART
      J=ND(I)
      DO 61 K=1,J
   61 D(K,I)=D(K,I)*DELX
      IFLAG=1
      IF(J.GT.2) GO TO 62
      V(I)=D(1,I)-D(J,I)
      GO TO 64
   62 V(I)=D(1,I)-D(2,I)
      JM1=J-1
      DO 63 K=1,JM1
      KP1=K+1
      DO 63 L=KP1,J
      CS=D(K,I)-D(L,I)
      IF(ABS(CS).GT.ABS(V(K))) GO TO 63
      V(I)=CS
      IFLAG=K
   63 CONTINUE
   64 WRITE(6,108) AA(I),XC(I),V(I),(D(K,I),K=1,J)
   65 X(I)=D(IFLAG,I)
      DO 66 I=LMSP,LX
      X(I)=0.
      AA(I)=(I-1)*DELX+XSTART
   66 WRITE(6,108) AA(I),XC(I)
      CALL DPLOT(D,4,NC,LX,-1,1,DELX,DSCAL,0.)
  107 FORMAT(1HO,'PRIMARY RESULT',//,'  LOCATION',5X,'ANOMALY',3X,
     1       'HILBERT',4X,'DIF',6X,'DEPTH1',3X,'DEPTH2...'/)
  108 FORMAT(2H  ,F7.2,2X,2F10.2,3X,F7.3,6(3X,F6.3))
      IF(IPUN.EQ.1) WRITE(7,111)(AA(I),XC(I),X(I),V(I),I=1,LX)
  111 FORMAT(5F10.3)
      STOP
      END
```

# APPENDIX III

## SAMPLE DATA SET

The following data set is used to illustrate the interpretation procedure. The output produced by this data set is given in Appendix IV.

```
B-25 CONSTANT DELT
 .5        114   15    1    0
   200.00       0.50
(5(8X,F8.1))
     0.0 48675.0     0.5 48650.0     1.0 48787.0     1.5 48960.0     2.0 48900.0
     2.5 48435.0     3.0 48630.0     3.5 49135.0     4.0 49000.0     4.5 48800.0
     5.0 48650.0     5.5 48550.0     6.0 48465.0     6.5 48395.0     7.0 48337.0
     7.5 48300.0     8.0 48286.0     8.5 48284.0     9.0 48282.0     9.5 48278.0
    10.0 48277.0    10.5 48285.0    11.0 48305.0    11.5 48333.0    12.0 48368.0
    12.5 48404.0    13.0 48435.0    13.5 48470.0    14.0 48505.0    14.5 48550.0
    15.0 48587.0    15.5 48589.0    16.0 48556.0    16.5 48513.0    17.0 48478.0
    17.5 48440.0    18.0 48400.0    18.5 48370.0    19.0 48344.0    19.5 48327.0
    20.0 48318.0    20.5 48314.0    21.0 48316.0    21.5 48324.0    22.0 48335.0
    22.5 48353.0    23.0 48382.0    23.5 48417.0    24.0 48450.0    24.5 48470.0
    25.0 48475.0    25.5 48465.0    26.0 48445.0    26.5 48430.0    27.0 48423.0
    27.5 48430.0    28.0 48445.0    28.5 48464.0    29.0 48473.0    29.5 48472.0
    30.0 48462.0    30.5 48452.0    31.0 48448.0    31.5 48450.0    32.0 48455.7
    32.5 48460.0    33.0 48458.3    33.5 48451.5    34.0 48442.0    34.5 48431.9
    35.0 48422.3    35.5 48414.1    36.0 48407.7    36.5 48403.0    37.0 48400.3
    37.5 48400.6    38.0 48403.9    38.5 48410.0    39.0 48421.0    39.5 48440.0
    40.0 48475.0    40.5 48535.9    41.0 48619.9    41.5 48690.0    42.0 48726.0
    42.5 48731.0    43.0 48722.0    43.5 48700.0    44.0 48673.0    44.5 48652.0
    45.0 48639.0    45.5 48635.0    46.0 48645.0    46.5 48663.0    47.0 48667.0
    47.5 48663.0    48.0 48673.0    48.5 48700.0    49.0 48754.9    49.5 48825.9
    50.0 48845.0    50.5 48795.1    51.0 48738.0    51.5 48718.0    52.0 48654.1
    52.5 48605.0    53.0 48602.0    53.5 48608.0    54.0 48639.0    54.5 48566.6
    55.0 48564.9    55.5 48629.9    56.0 48687.9    56.5 48807.8
```

# APPENDIX IV

## SAMPLE OUTPUT

```
B-25 CONSTANT DELT

INPUT PARAMETERS
  DELX= 0.5000000   LX=  114   IW=   15   ILINE=    1   IPUN=    0

PREDICTION FILTER

1.0000000-1.5121580 1.4560782-1.6133685 1.3634520-1.3632970 1.3925827-1.1658333 0.9808939-0.7546977 0.5962985-0.4361612
0.3314574-0.2251094 0.0987948-0.0526878

PREDICTED EXTENSION

   193.58    -9.10   139.12   -10.75   163.50   -19.01   180.04    14.01   177.66    55.35   143.77    87.77
   116.73    82.94   115.25    88.34    99.85   107.90    71.31   116.07    45.36   108.96    30.21    97.00
    20.07    86.80    12.92    77.77     5.01    69.76    -0.73    56.76     1.21    46.05     2.28    39.92
     4.23    33.16     7.12    29.13     9.78    24.95    14.50    23.10    17.24    23.79    19.00    24.21
    20.48    25.56    20.65    27.22    20.38    28.73    19.14    30.42    17.32    31.33    15.23    31.98
    12.93    31.97    10.56    31.68     8.24    30.68     6.20    29.46     4.38    27.77     2.98    25.99
     1.92    24.03     1.16    22.15     0.81    20.21     0.65    18.61     0.73    16.94     0.95    15.73
     1.23    14.49     1.58    13.66     1.89    12.81     2.15    12.30     2.34    11.70     2.44    11.40
     2.45    10.91     2.38    10.68     2.23    10.19     2.03     9.92     1.78     9.35     1.52     9.01
     1.25     8.34     1.00     7.91     0.77     7.16     0.58     6.67     0.42     5.87     0.30     5.37
     0.22     4.56     0.17     4.08     0.15     3.28     0.15     2.84     0.17     2.08     0.19     1.69
     0.22     0.96     0.25     0.61     0.27    -0.10     0.29    -0.43     0.29    -1.17     0.34    -1.53
     0.40    -2.26     0.45    -2.57     0.51    -3.29     0.56    -3.59     0.60    -4.31     0.64    -4.59
     0.67    -5.33     0.68    -5.61     0.69    -6.39     0.68    -6.70     0.68    -7.54     0.67    -7.90
     0.67    -5.82     0.68    -9.25     0.72   -10.25     0.80   -10.75     0.92   -11.84     1.08   -12.37
     1.31   -13.52     1.60   -14.06     1.95   -15.21     2.35   -15.69     2.79   -16.79     3.27   -17.17
     3.74   -18.17     4.21   -18.43     4.62   -19.33     4.98   -19.52     5.27   -20.38     5.40   -20.56
     5.51   -21.57     5.41   -21.84     5.28   -23.24     5.15   -23.83     4.83   -25.66     4.82   -26.90
     4.73   -29.19     4.97   -31.15     5.65   -33.97     6.40   -36.20     7.94   -39.63     9.87   -41.87
    12.41   -45.12    15.30   -46.94    18.85   -49.81    22.87   -50.58    27.06   -52.28    31.78   -51.07
    34.32   -50.81    38.54   -50.33    41.92   -47.66    42.93   -45.72    45.36   -43.02    41.16   -40.46
    43.25   -45.83    46.20   -38.97    37.42   -38.38    32.10   -43.52    26.67   -55.28    35.16   -69.13
    42.23   -66.74    29.97   -73.58    31.12  -105.51    62.75  -131.79   101.80  -122.63   100.95  -103.34
    91.76  -119.32    95.92  -170.60   208.73  -235.30   335.40  -105.94

PRIMARY RESULT

 LOCATION      ANOMALY    HILBERT      DIF      DEPTH1   DEPTH2...

     0.00       227.41      -4.62
     0.50       201.02    -114.94
     1.00       336.62    -147.34
     1.50       508.22     -30.04
     2.00       446.82     321.64
     2.50       -19.57     245.27
     3.00       174.03    -263.66
     3.50       677.63      -2.58    0.000    0.393
     4.00       541.24     408.41    0.000    0.492
     4.50       339.84     488.19    0.000    0.604
     5.00       186.44     511.23    0.000    0.716
     5.50        87.05     481.26    0.000    0.829
     6.00         0.65     463.62    0.000    0.962
     6.50       -70.75     417.96   -0.164    1.148    1.202
     7.00      -130.14     373.57   -0.095    1.401    1.432
     7.50      -168.54     308.27   -0.054    1.721    1.739
     8.00      -183.94     255.39   -0.019    1.866    1.873
     8.50      -187.33     208.30   -0.006    1.967    1.969
     9.00      -190.73     176.98    0.049    1.982    1.966
     9.50      -196.13     140.53    0.049    1.956    1.940
    10.00      -198.53     104.61    0.100    1.898    1.877    1.831
    10.50      -191.92      61.22    0.100    1.793    1.772    1.727
    11.00      -173.32      24.69    0.120    1.658    1.632    1.578
    11.50      -146.72      -7.42    0.132    1.456    1.427    1.368
    12.00      -113.11     -27.94    0.169    1.252    1.213    1.139
    12.50       -78.51     -37.39    0.224    1.057    1.005    0.907
    13.00       -48.91     -40.17    0.474    0.886    0.817    0.679    0.412
    13.50       -15.30     -40.47    0.758    0.758    0.671    0.486    0.000
    14.00        18.30     -32.13    0.700    0.700    0.604    0.393    0.000
    14.50        61.90     -14.14    0.710    0.710    0.618    0.425    0.000
```

| | | | | | | | |
|---|---|---|---|---|---|---|---|
| 15.00 | 97.51 | 37.93 | 0.580 | 0.781 | 0.702 | 0.546 | 0.202 |
| 15.50 | 98.11 | 103.53 | 0.405 | 0.900 | 0.835 | 0.712 | 0.496 |
| 16.00 | 63.71 | 157.25 | 0.319 | 1.060 | 1.008 | 0.908 | 0.740 |
| 16.50 | 19.32 | 179.71 | 0.256 | 1.245 | 1.205 | 1.124 | 0.989 |
| 17.00 | -17.08 | 190.84 | 0.211 | 1.407 | 1.375 | 1.308 | 1.196 |
| 17.50 | -56.48 | 196.52 | 0.178 | 1.542 | 1.515 | 1.458 | 1.365 |
| 18.00 | -97.87 | 188.12 | 0.171 | 1.671 | 1.645 | 1.590 | 1.500 |
| 18.50 | -129.27 | 168.95 | 0.175 | 1.811 | 1.786 | 1.728 | 1.636 |
| 19.00 | -156.67 | 146.75 | 0.184 | 1.943 | 1.915 | 1.853 | 1.759 |
| 19.50 | -175.07 | 116.47 | 0.180 | 2.055 | 2.024 | 1.964 | 1.875 |
| 20.00 | -185.46 | 88.50 | 0.171 | 2.103 | 2.073 | 2.016 | 1.931 |
| 20.50 | -190.86 | 58.74 | 0.163 | 2.093 | 2.064 | 2.010 | 1.931 |
| 21.00 | -190.26 | 30.41 | 0.148 | 2.064 | 2.038 | 1.989 | 1.917 |
| 21.50 | -183.65 | 2.90 | 0.124 | 2.012 | 1.990 | 1.949 | 1.888 |
| 22.00 | -174.05 | -21.42 | 0.094 | 1.919 | 1.902 | 1.871 | 1.825 |
| 22.50 | -157.45 | -47.99 | 0.060 | 1.803 | 1.792 | 1.771 | 1.743 |
| 23.00 | -129.84 | -66.97 | 0.031 | 1.678 | 1.670 | 1.657 | 1.647 |
| 23.50 | -96.24 | -73.76 | 0.002 | 1.542 | 1.535 | 1.530 | 1.539 |
| 24.00 | -64.64 | -62.85 | -0.038 | 1.413 | 1.410 | 1.414 | 1.451 |
| 24.50 | -46.03 | -40.53 | -0.085 | 1.303 | 1.303 | 1.319 | 1.389 |
| 25.00 | -42.43 | -15.22 | -0.136 | 1.231 | 1.235 | 1.264 | 1.366 |
| 25.50 | -53.83 | 5.64 | -0.193 | 1.222 | 1.233 | 1.278 | 1.415 |
| 26.00 | -75.22 | 11.57 | -0.235 | 1.292 | 1.311 | 1.370 | 1.527 |
| 26.50 | -91.62 | 2.73 | -0.271 | 1.396 | 1.424 | 1.495 | 1.667 |
| 27.00 | -100.02 | -13.75 | -0.333 | 1.495 | 1.534 | 1.625 | 1.828 |
| 27.50 | -94.42 | -31.85 | -0.430 | 1.588 | 1.644 | 1.765 | 2.019 |
| 28.00 | -80.81 | -41.43 | -0.566 | 1.674 | 1.750 | 1.911 | 2.240 |
| 28.50 | -63.21 | -39.81 | -0.700 | 1.772 | 1.870 | 2.069 | 2.471 |
| 29.00 | -55.61 | -26.32 | -0.805 | 1.901 | 2.018 | 2.250 | 2.706 |
| 29.50 | -58.00 | -14.57 | -0.972 | 2.067 | 2.212 | 2.495 | 3.039 |
| 30.00 | -69.40 | -6.89 | -1.149 | 2.250 | 2.423 | 2.759 | 3.399 |
| 30.50 | -80.80 | -11.47 | -1.208 | 2.458 | 2.648 | 3.007 | 3.665 |
| 31.00 | -86.19 | -18.99 | -1.255 | 2.679 | 2.885 | 3.262 | 3.934 |
| 31.50 | -85.59 | -27.76 | -1.190 | 2.873 | 3.081 | 3.445 | 4.064 |
| 32.00 | -81.29 | -30.45 | -0.967 | 3.055 | 3.237 | 3.538 | 4.022 |
| 32.50 | -78.38 | -28.60 | -0.752 | 3.192 | 3.345 | 3.582 | 3.944 |
| 33.00 | -81.48 | -22.84 | -0.508 | 3.217 | 3.327 | 3.489 | 3.726 |
| 33.50 | -89.68 | -20.93 | -0.261 | 3.255 | 3.316 | 3.400 | 3.515 |
| 34.00 | -100.57 | -21.56 | -0.165 | 3.208 | 3.248 | 3.301 | 3.374 |
| 34.50 | -112.07 | -27.82 | -0.076 | 3.159 | 3.181 | 3.206 | 3.235 |
| 35.00 | -123.07 | -36.32 | -0.026 | 3.074 | 3.085 | 3.093 | 3.100 |
| 35.50 | -132.66 | -49.49 | 0.021 | 2.980 | 2.980 | 2.973 | 2.959 |
| 36.00 | -140.46 | -63.76 | 0.040 | 2.829 | 2.825 | 2.812 | 2.789 |
| 36.50 | -146.56 | -81.72 | 0.055 | 2.642 | 2.635 | 2.617 | 2.587 |
| 37.00 | -150.66 | -100.91 | 0.058 | 2.398 | 2.391 | 2.372 | 2.341 |
| 37.50 | -151.75 | -124.02 | 0.059 | 2.173 | 2.168 | 2.150 | 2.115 |
| 38.00 | -149.85 | -147.42 | 0.057 | 2.024 | 2.020 | 2.003 | 1.967 |
| 38.50 | -145.15 | -175.24 | 0.060 | 1.912 | 1.907 | 1.889 | 1.852 |
| 39.00 | -135.54 | -205.66 | 0.064 | 1.820 | 1.814 | 1.794 | 1.756 |
| 39.50 | -117.94 | -242.95 | 0.080 | 1.733 | 1.722 | 1.697 | 1.652 |
| 40.00 | -84.34 | -282.77 | 0.098 | 1.649 | 1.634 | 1.604 | 1.551 |
| 40.50 | -24.83 | -317.94 | 0.111 | 1.577 | 1.560 | 1.524 | 1.466 |
| 41.00 | 57.77 | -317.73 | 0.118 | 1.527 | 1.507 | 1.470 | 1.409 |
| 41.50 | 126.47 | -275.18 | 0.113 | 1.501 | 1.481 | 1.444 | 1.388 |
| 42.00 | 161.08 | -213.03 | 0.094 | 1.496 | 1.478 | 1.447 | 1.402 |
| 42.50 | 164.68 | -157.45 | 0.066 | 1.503 | 1.489 | 1.466 | 1.436 |
| 43.00 | 154.28 | -113.89 | 0.029 | 1.516 | 1.508 | 1.496 | 1.487 |
| 43.50 | 130.89 | -81.80 | -0.025 | 1.538 | 1.540 | 1.545 | 1.563 |
| 44.00 | 102.49 | -68.67 | -0.076 | 1.588 | 1.605 | 1.639 | |
| 44.50 | 80.09 | -70.06 | -0.176 | 1.693 | 1.734 | 1.811 | |
| 45.00 | 65.69 | -79.18 | -0.288 | 1.848 | 1.918 | 2.039 | |
| 45.50 | 60.30 | -93.98 | -0.398 | 1.953 | 2.054 | 2.219 | |
| 46.00 | 68.90 | -108.63 | -0.470 | 1.816 | 1.932 | 2.130 | |
| 46.50 | 85.50 | -108.60 | -0.486 | 1.622 | 1.740 | 1.946 | |
| 47.00 | 88.11 | -99.30 | -0.332 | 1.493 | 1.604 | | |
| 47.50 | 82.71 | -105.56 | -0.286 | 1.399 | 1.494 | | |
| 48.00 | 91.31 | -123.40 | -0.220 | 1.309 | 1.383 | | |
| 48.50 | 116.92 | -141.39 | -0.125 | 1.197 | 1.238 | | |
| 49.00 | 170.42 | -149.06 | -0.054 | 1.099 | 1.117 | | |
| 49.50 | 240.02 | -103.76 | 0.000 | 1.032 | 1.032 | | |
| 50.00 | 257.73 | -8.45 | 0.018 | 0.993 | 0.987 | | |
| 50.50 | 206.43 | 65.25 | 0.000 | 0.982 | | | |
| 51.00 | 147.93 | 76.67 | 0.000 | 0.958 | | | |
| 51.50 | 126.54 | 89.81 | 0.000 | 0.866 | | | |
| 52.00 | 61.24 | 110.35 | 0.000 | 0.748 | | | |
| 52.50 | 10.74 | 59.90 | 0.000 | 0.646 | | | |
| 53.00 | 6.34 | 26.93 | 0.000 | 0.546 | | | |
| 53.50 | 10.95 | -12.51 | | | | | |
| 54.00 | 40.55 | 6.65 | | | | | |
| 54.50 | -33.25 | 10.07 | | | | | |
| 55.00 | -36.34 | -96.49 | | | | | |
| 55.50 | 27.26 | -129.92 | | | | | |
| 56.00 | 83.86 | -167.72 | | | | | |
| 56.50 | 202.37 | -125.88 | | | | | |

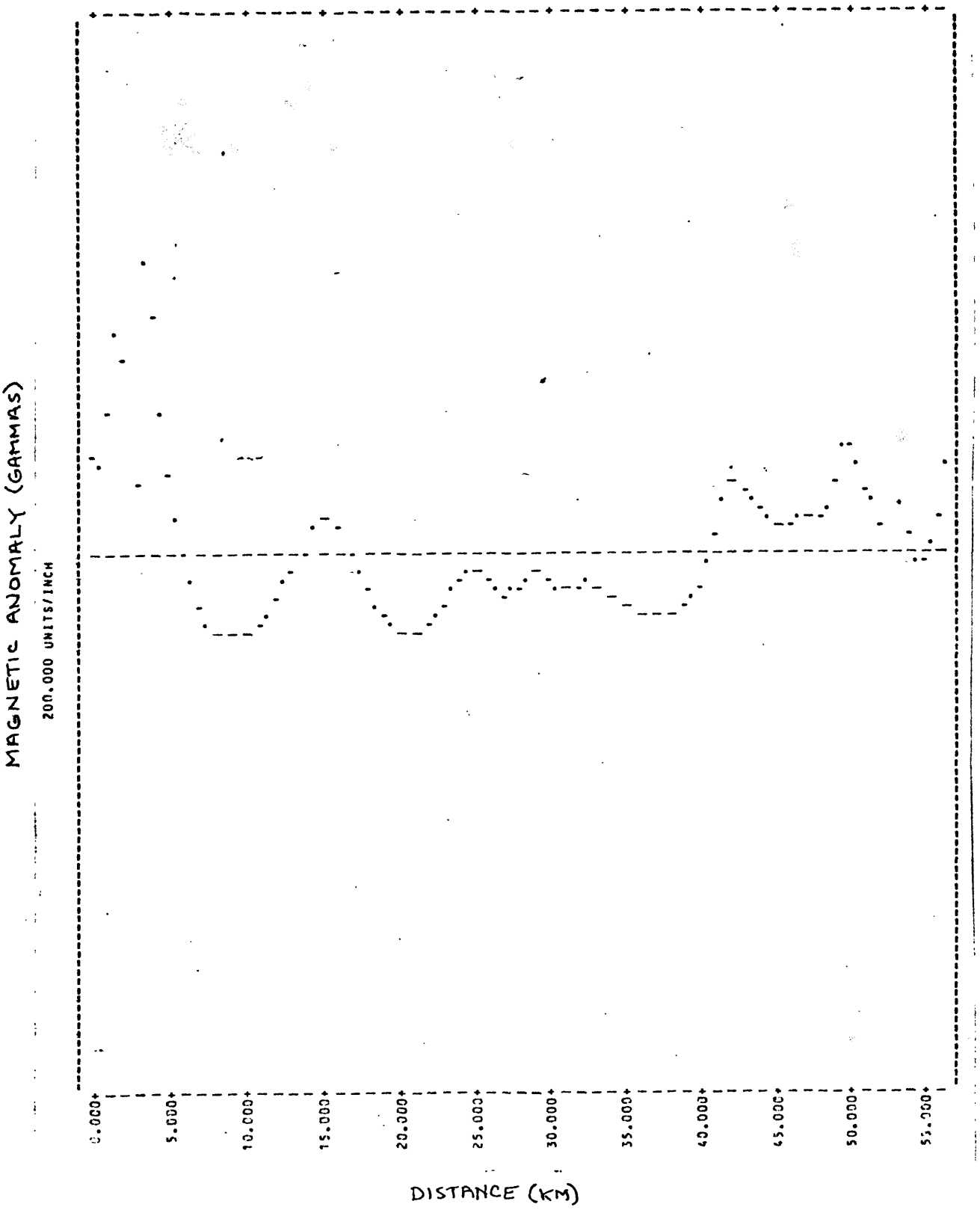
MAGNETIC ANOMALY (GAMMAS)
200.000 UNITS/INCH
0.000+
5.000+
10.000+
15.000+
20.000+
25.000+
30.000+
35.000+
40.000+
45.000+
50.000+
55.000+
DISTANCE (KM)

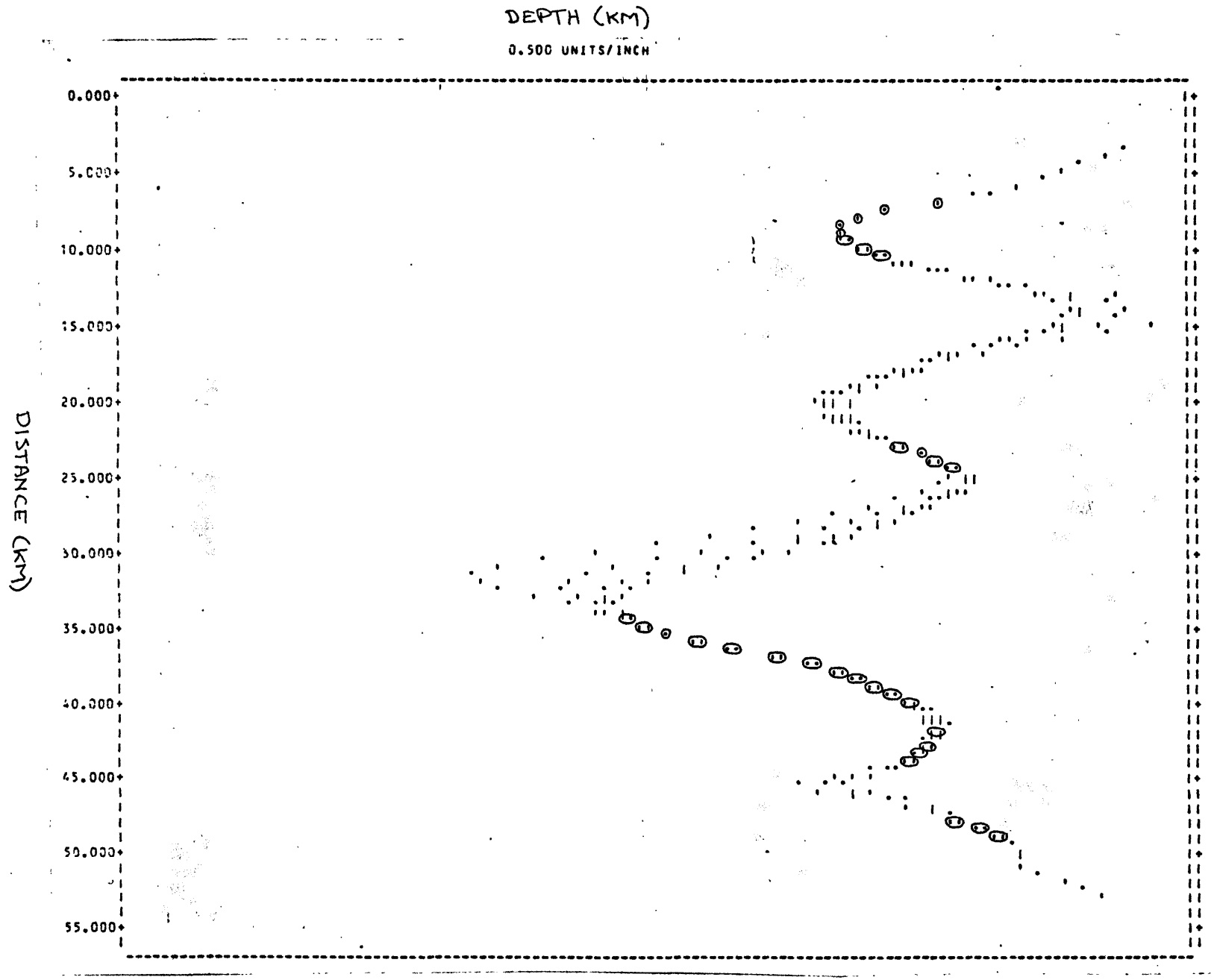
DEPTH (KM)
0.500 UNITS/INCH
0.000
5.000
10.000
15.000
20.000
25.000
30.000
35.000
40.000
45.000
50.000
55.000
DISTANCE (KM)

SECONDARY RESULT

| LOCATION | FLAG | DIF | DEPTH1 | DEPTH2... | |
|---|---|---|---|---|---|
| 6.50 | 1 | 0.000 | 0.870 | | |
| 7.00 | 1 | 0.000 | 1.144 | | |
| 7.50 | 1 | 0.000 | 1.484 | | |
| 8.00 | 1 | 0.000 | 1.758 | | |
| 8.50 | 1 | 0.000 | 1.923 | | |
| 9.00 | 1 | 0.000 | 2.448 | | |
| 9.50 | 1 | 0.000 | 2.411 | | |
| 10.00 | 1 | -0.347 | 2.493 | 2.840 | |
| 10.50 | 1 | -0.206 | 2.353 | 2.560 | |
| 11.00 | 1 | -0.207 | 2.281 | 2.488 | |
| 11.50 | 1 | -0.143 | 1.986 | 2.129 | |
| 12.00 | 1 | -0.098 | 1.808 | 1.907 | |
| 12.50 | 1 | -0.066 | 1.635 | 1.701 | |
| 13.00 | 2 | -0.016 | 1.499 | 1.563 | 1.579 |
| 13.50 | 1 | -0.041 | 1.361 | 1.401 | 1.082 |
| 14.00 | 1 | -0.015 | 1.265 | 1.279 | 0.738 |
| 14.50 | 1 | 0.014 | 1.250 | 1.236 | 0.839 |
| 15.00 | 1 | 0.021 | 1.326 | 1.305 | 1.239 |
| 15.50 | 1 | -0.010 | 1.465 | 1.475 | 1.446 |
| 16.00 | 2 | -0.052 | 1.647 | 1.735 | 1.787 |
| 16.50 | 2 | -0.143 | 1.825 | 2.012 | 2.154 |
| 17.00 | 2 | -0.190 | 1.956 | 2.197 | 2.387 |
| 17.50 | 2 | -0.192 | 2.067 | 2.308 | 2.500 |
| 18.00 | 2 | -0.203 | 2.277 | 2.593 | 2.796 |
| 18.50 | 2 | -0.291 | 2.548 | 3.100 | 3.391 |
| 19.00 | 2 | -0.318 | 2.995 | 3.873 | 4.191 |
| 19.50 | 2 | -0.215 | 3.514 | 4.282 | 4.498 |
| 20.00 | 2 | -0.156 | 3.657 | 4.191 | 4.347 |
| 20.50 | 2 | -0.113 | 3.486 | 3.872 | 3.986 |
| 21.00 | 2 | -0.092 | 3.162 | 3.415 | 3.507 |
| 21.50 | 2 | -0.046 | 2.769 | 2.917 | 2.963 |
| 22.00 | 2 | -0.013 | 2.371 | 2.449 | 2.461 |
| 22.50 | 1 | 0.003 | 2.049 | 2.074 | 2.046 |
| 23.00 | 1 | 0.016 | 1.825 | 1.808 | 1.737 |
| 23.50 | 1 | 0.049 | 1.631 | 1.581 | 1.470 |
| 24.00 | 1 | 0.075 | 1.452 | 1.377 | 1.228 |
| 24.50 | 1 | 0.096 | 1.305 | 1.209 | 1.025 |
| 25.00 | 1 | 0.109 | 1.199 | 1.090 | 0.880 |
| 25.50 | 1 | 0.117 | 1.141 | 1.024 | 0.794 |
| 26.00 | 1 | 0.116 | 1.145 | 1.030 | 0.795 |
| 26.50 | 1 | 0.110 | 1.168 | 1.058 | 0.826 |
| 27.00 | 1 | 0.106 | 1.158 | 1.052 | 0.818 |
| 27.50 | 1 | 0.108 | 1.121 | 1.012 | 0.767 |
| 28.00 | 1 | 0.117 | 1.066 | 0.949 | 0.677 |
| 28.50 | 1 | 0.116 | 1.021 | 0.903 | 0.612 |
| 29.00 | 1 | 0.116 | 1.004 | 0.887 | 0.591 |
| 29.50 | 1 | 0.119 | 0.972 | 0.852 | 0.546 |
| 30.00 | 1 | 0.126 | 0.951 | 0.825 | 0.505 |
| 30.50 | 1 | 0.114 | 0.962 | 0.848 | 0.554 |
| 31.00 | 1 | 0.103 | 0.979 | 0.876 | 0.606 |
| 31.50 | 1 | 0.075 | 1.015 | 0.940 | 0.713 |
| 32.00 | 1 | 0.037 | 1.122 | 1.085 | 0.913 |
| 32.50 | 1 | -0.007 | 1.250 | 1.257 | 1.135 |
| 33.00 | 1 | 0.020 | 1.447 | 1.499 | 1.426 |
| 33.50 | 2 | 0.010 | 1.819 | 1.941 | 1.931 |
| 34.00 | 2 | -0.005 | 2.075 | 2.205 | 2.210 |
| 34.50 | 2 | -0.073 | 2.383 | 2.575 | 2.648 |
| 35.00 | 2 | -0.092 | 2.655 | 2.848 | 2.939 |
| 35.50 | 2 | -0.133 | 2.964 | 3.204 | 3.357 |
| 36.00 | 2 | -0.133 | 3.024 | 3.235 | 3.369 |
| 36.50 | 2 | -0.117 | 2.979 | 3.172 | 3.289 |
| 37.00 | 2 | -0.107 | 2.664 | 2.857 | 2.963 |
| 37.50 | 2 | -0.161 | 2.316 | 2.525 | 2.706 |
| 38.00 | 1 | -0.182 | 2.119 | 2.301 | 2.490 |
| 38.50 | 1 | -0.151 | 2.019 | 2.170 | 2.338 |
| 39.00 | 1 | -0.120 | 1.956 | 2.075 | 2.212 |
| 39.50 | 1 | -0.107 | 1.935 | 2.042 | 2.166 |
| 40.00 | 1 | -0.093 | 1.914 | 2.007 | 2.116 |
| 40.50 | 1 | -0.078 | 1.887 | 1.965 | 2.060 |
| 41.00 | 1 | -0.061 | 1.857 | 1.918 | 1.993 |
| 41.50 | 1 | -0.041 | 1.818 | 1.860 | 1.902 |
| 42.00 | 2 | -0.005 | 1.765 | 1.786 | 1.791 |
| 42.50 | 1 | -0.004 | 1.701 | 1.705 | 1.679 |
| 43.00 | 1 | 0.012 | 1.623 | 1.612 | 1.559 |
| 43.50 | 1 | 0.022 | 1.519 | 1.496 | 1.431 |
| 44.00 | 1 | 0.035 | 1.394 | 1.359 | |
| 44.50 | 1 | 0.047 | 1.270 | 1.223 | |
| 45.00 | 1 | 0.033 | 1.173 | 1.140 | |
| 45.50 | 1 | 0.022 | 1.081 | 1.059 | |
| 46.00 | 1 | 0.046 | 0.976 | 0.930 | |
| 46.50 | 1 | 0.056 | 0.896 | 0.840 | |
| 47.00 | 1 | 0.000 | 0.865 | | |
| 47.50 | 1 | 0.000 | 0.869 | | |
| 48.00 | 1 | 0.000 | 0.896 | | |
| 48.50 | 1 | 0.000 | 0.952 | | |
| 49.00 | 1 | 0.000 | 0.992 | | |
| 49.50 | 1 | 0.000 | 1.033 | | |
| 50.00 | 1 | 0.000 | 1.028 | | |

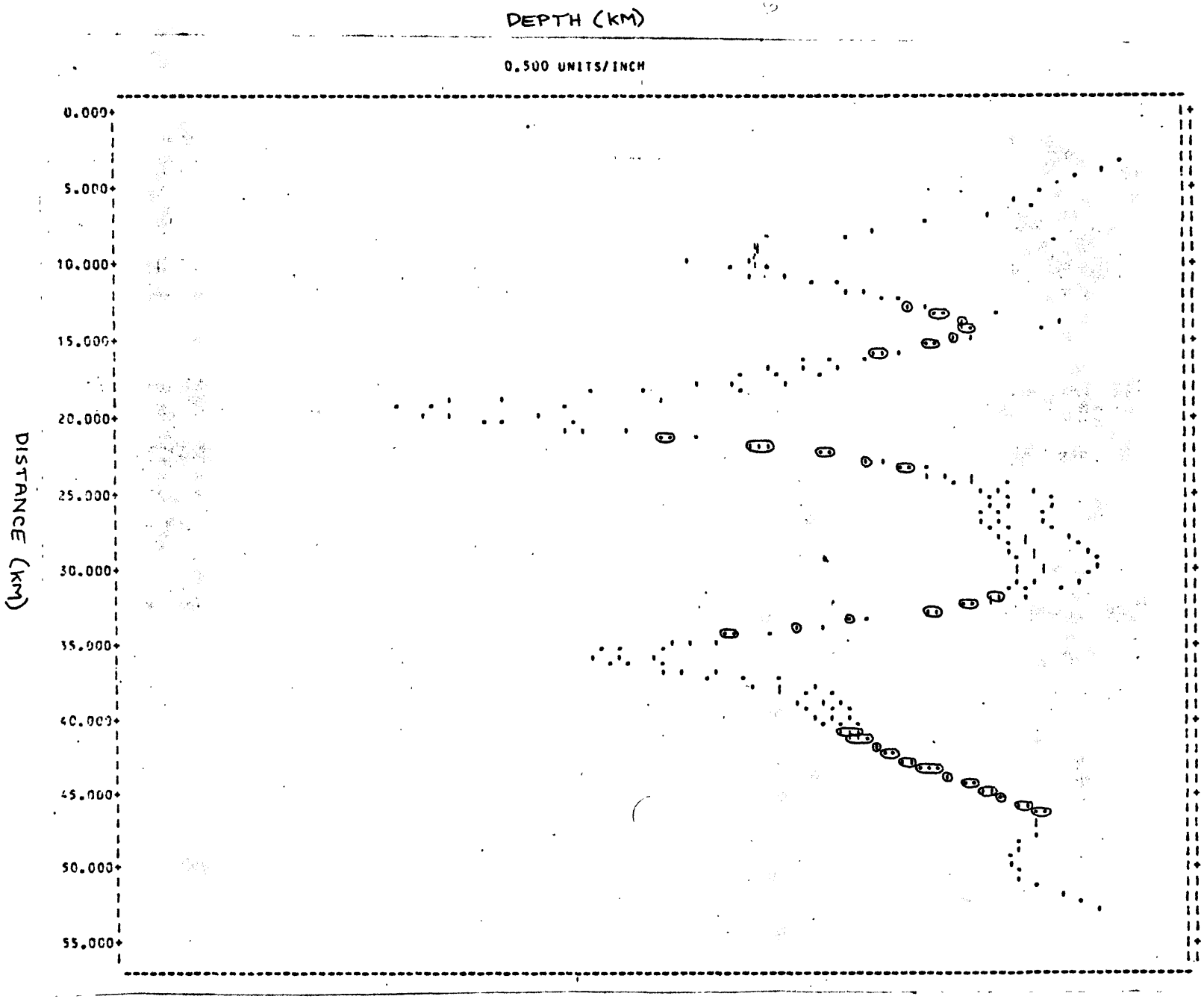
DEPTH (KM)
0.500 UNITS/INCH
0.000
5.000
10.000
15.000
20.000
25.000
30.000
35.000
40.000
45.000
50.000
55.000
DISTANCE (KM)